A protective role of REM sleep in the pathological basal ganglia-cortical circuit of Parkinson's disease

Jin-Xiao Zhang[1], Clay Smyth[2], Md Fahim Anjum[1], Yue Leng[3], Andrew D. Krystal[3], Philip A. Starr[4], Simon Little[1]

[1]Department of Neurology, University of California, San Francisco
[2]Department of Bioengineering, University of California, San Francisco
[3]Department of Psychiatry, University of California, San Francisco
[4]Department of Neurological Surgery, University of California, San Francisco

Abstract

Sleep disturbance is involved in the progression of neurodegenerative diseases, but the neurophysiological mechanisms remain unclear in humans. We recorded sleep at home using portable polysomnography for multiple nights in patients with Parkinson's disease implanted with sensing DBS, capturing intracranial neural signals from both the basal ganglia and motor cortex. We found that longer duration and shorter latency of rapid eye movement (REM) sleep predicted reduced next-morning neural signatures known to be pathological, including resting beta oscillations and hyper-neural connectivity between basal ganglia and motor cortex. Moreover, within REM sleep, stronger cortical delta activity particularly predicted reduced pathological neural signatures. Computational modeling of the evoked potential response in the basal-cortical circuit revealed that REM delta activity was associated with not only the amplitude of the evoked response, but also its natural oscillatory and decaying properties, suggesting REM sleep-mediated neural plasticity. The anti-relationship between delta activity and morning pathological neural signals was found to be primarily driven by the amplitude of delta waves, and less by their occurrence rate. In addition, as the REM sleep percentage and REM delta power increased in later hours during sleep, their protective effects also increased. Overall, our findings highlight the potential protective roles of REM sleep and its associated slow-wave activity in the neurophysiological health of Parkinson's disease.

Sleep disturbance is commonly associated with a broad range of neurodegenerative diseases, including Parkinson's disease (PD), Alzheimer's disease (AD), vascular dementia (VaD), frontotemporal dementia (FTD), dementia with Lewy bodies (LBD), and Huntington disease (HD) (Musiek and Holtzman 2016; Shi et al. 2018; Porter, Buxton, and Avidan 2015). Increasing evidence has shown that sleep disturbances may happen early in the disease course and precede the onset of more typical symptoms of these neurodegenerative diseases (Schenck, Boeve, and Mahowald 2013; He, Hu, and Jiang 2020; Irwin and Vitiello 2019; Rothman and Mattson 2012). More importantly, recent evidence suggests that sleep disturbances could contribute to the pathogenesis of neurodegenerative diseases (Shokri-Kojori et al. 2018; Owen and Veasey 2020; Owen et al. 2021). Although animal research has shed light on some cellular and molecular mechanisms linking sleep disturbance to neurodegenerative diseases (Musiek and Holtzman 2016; C.-W. Chen et al. 2023), the neurophysiological mechanisms of this link in humans remain less understood. Given the wide presence of sleep disturbance in neurodegeneration diseases, a neurophysiological understanding of this link may facilitate identifying intervention targets during sleep for preventing and slowing neurodegeneration disease.

Human sleep is broadly classified into alternating stages of non-rapid eye movement (NREM) sleep and rapid eye movement (REM) sleep. Electroencephalogram (EEG) in NREM sleep is hallmarked by larger-amplitude lower-frequency delta (1–4Hz) activity, especially during the deep NREM stage (i.e., N3) (Berry et al. 2017). During REM sleep, EEG transitions to a low-amplitude mixed-frequency desynchronized activity, similar to wakeful EEG. Although the neurophysiological activity during REM is generally faster compared to NREM, recent evidence has shown the existence of slow-wave delta activity during REM sleep in both humans and mice, particularly in the frontal-central region (Bernardi et al. 2019; Funk et al. 2016). Importantly, slow-wave sleep has been shown in animals to be beneficial in multiple domains, including glymphatic clearance (Xie et al. 2013) and neuroinflammation reduction (Wisor, Schmidt, and Clegern 2011; Zielinski and Gibbons 2022). In the context of human neurodegenerative diseases, slow-wave neural activity during sleep is associated with slower motor progression in PD (Schreiner et al. 2019; J. Chen et al. 2024), and better memory functions and slower accumulation of pathological beta-amyloid in AD (Wunderlin et al. 2020; Lee et al. 2020; Ju et al. 2017). Most studies on the role of slow-wave activity in neurodegenerative diseases have focused on NREM sleep and it remains unclear how the effect of slow-wave activity applies to REM sleep.

PD is a neurodegeneration condition closely related to sleep disturbance (Zahed et al. 2021). Over 80% of REM sleep behavior disorder (RBD) patients were found to develop PD or neurodegenerative dementia eventually (Schenck, Boeve, and Mahowald 2013). Certain therapies for Parkinson's Disease, such as deep brain stimulation (DBS) with sensing capacity, provide a unique means of directly studying the neurophysiology of PD in a chronic and ecologically valid manner (Gilron et al. 2021). Thus, compared to other neurodegenerative diseases, PD provides a valuable window to study the neurophysiological mechanism of the sleep-neurodegeneration link in a within-subject manner. This is particularly important given that

most human studies on the role of sleep in neurodegeneration have relied on a between-subject approach (Schreiner et al. 2019; J. Chen et al. 2024).

During daytime, PD is characterized by pathological neural signatures in the basal ganglia (BG)-motor cortex network, prominently the excessive activity and connectivity at beta (13-30 Hz) band (Hammond, Bergman, and Brown 2007; Little and Brown 2014; Uhlhaas and Singer 2006; Moran et al. 2011; Little et al. 2013). These pathological neural signatures predict motor symptoms in PD patients and are important indices of disease progression (Little et al. 2012; C. C. Chen et al. 2010; Morelli and Summers 2023; Neumann et al. 2017; Stoffers et al. 2008). Given the role of sleep in shaping neural connectivity in various brain networks (Verweij et al. 2014; Tashjian et al. 2018; Di et al. 2024), we expect that sleep disturbance would also influence the neural connectivity of the BG-motor cortex network in PD patients. Specifically, we hypothesize that stronger delta slow-wave activity during sleep is associated with reduced pathological neural signatures in the basal-cortical network after sleep. Given the pathological role of beta oscillations in PD, we expect that stronger beta activity during sleep is associated with the opposite results. Considering the precursory role of REM sleep behavior disorder in PD (Schenck, Boeve, and Mahowald 2013) and prior findings regarding NREM sleep (Schreiner et al. 2019; J. Chen et al. 2024), we herein test both the effects of REM and NREM sleep and directly compare them in this study. We investigate a unique cohort of patients which chronically implanted sensorimotor cortical electrocorticography (ECoG) and basal ganglia electrode implants. Through a novel architecture whereby patients can stream neural data for the whole night while at home, we present the first study of within-participant, multi-night, at-home, intracranial cortico-basal sleep recordings in PD patients in relation to daytime pathological neural network signatures.

Results

In four patients with PD, we obtained neurophysiological recordings during nighttime sleep and the subsequent morning for multiple nights. These patients are implanted with bilateral intracranial ECoG strips spanning the central sulcus and DBS leads at the basal ganglia (subthalamic nucleus, STN, or globus pallidus internus, GPi) (Figure 1A). Cortical and subcortical electrodes are capable of chronically sensing local field potentials (Figure 1B). The nighttime intracranial recordings were obtained along with portable extracranial polysomnography (PSG) and were scored into REM or NREM 1-3 stages by a machine learning algorithm (Arnal et al. 2020; González et al. 2024). The morning recordings included both passive multi-site resting state recordings (local and functional connectivity) and an evoked potential (EP) paradigm to assess effective neural connectivity. We used linear mixed-effects (LME) models to test how sleep attributes may predict next-morning neural network features. In order to test and compare the effects of an attribute of REM and NREM sleep, we included them in the same LME model. In a series of ‘duration’ models, we tested the effects of the duration and onset latency of REM and NREM sleep. In a series of ‘power’ models, we tested the effects of delta and beta power during REM and NREM sleep (see Supplementary Figures 2-5 for exploratory results with all power bands).

Overnight sleep and sleep neurophysiology

Participants' intracranial cortical and subcortical signals were recorded for approximately ten nights (total *n*=39). They also wore a portable scalp PSG (DREEM2) for quantifications of sleep durations and automated hypnogram generation (Figure 1C) (Arnal et al 2020). Participants received continuous, therapeutic DBS while sleeping. On average, participants slept for 6.1±1.1 hours each night and achieved 79.9% (SD=7.8%) sleep efficiency. According to scored hypnograms (Figure 1F), participants spent 22.0% (SD=8.3%) of their sleep during REM stage and 68.8% (SD=8.5%) during NREM (N2 and N3) stages. As expected, the REM sleep percentage was greater and the NREM sleep percentage was smaller in the later half of the night than the first half (Figure 1H). We calculated the spectral power of cortical channels during REM and NREM stages (Figure 1G). Similar to healthy individuals, our PD participants typically had higher power in the delta band and lower power in higher frequency bands (beta and above) during NREM than REM sleep.

After awakening and before taking medications, participants completed a standardised morning evaluation session, including a resting-state recording section and then an automated BG → cortical EP recording (Figure 1D, 1E). The morning session facilitated an assessment of pathological neural network features in the BG-motor cortex circuit.

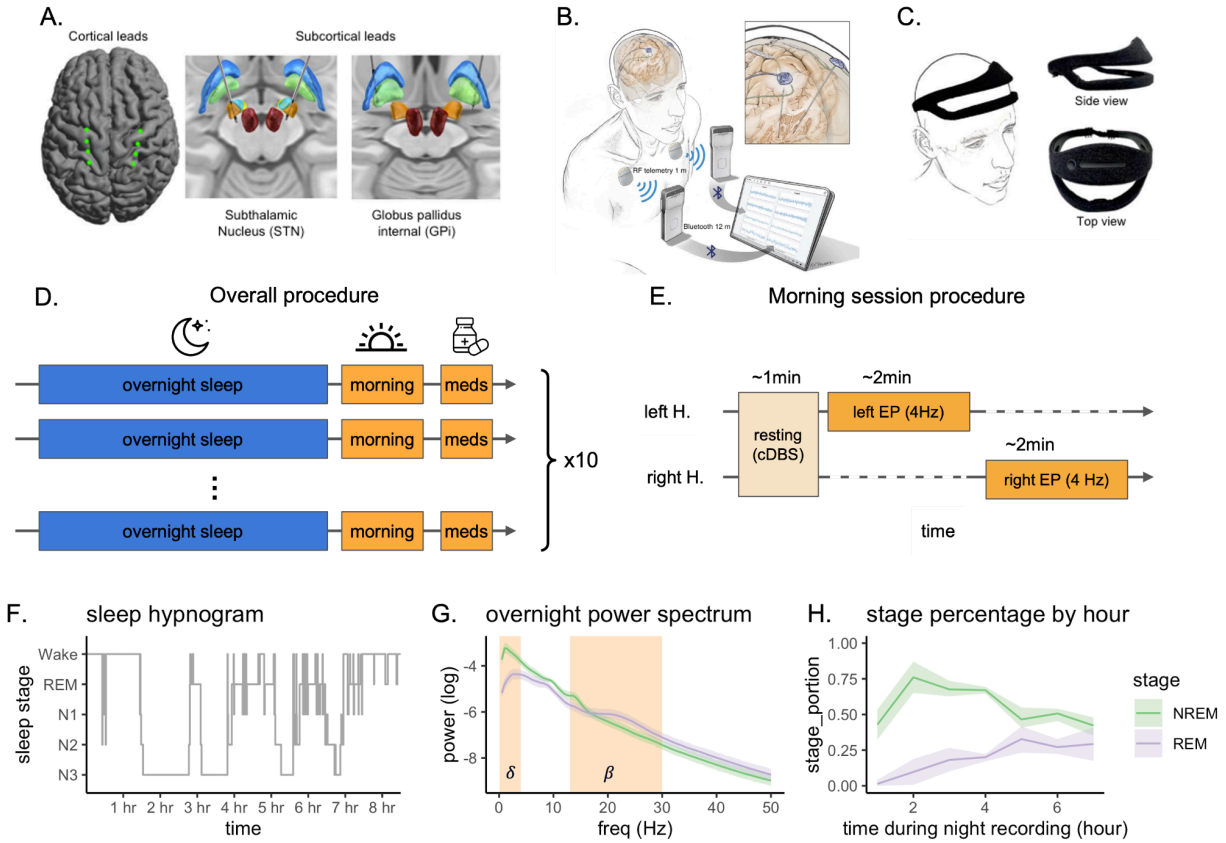

Figure 1. Study overview. (A) Illustrations of the placement of the RC+S electrodes in the sensorimotor cortex and subcortical basal ganglia. (B) Schematic of the intracranial RC+S system setup of streaming data wirelessly. (C) Portable polysomnography using the DREEM2

headband. (D) An overview of the multi-night-morning protocol containing an overnight recording session and a morning recording session for approximately 10 days. Morning sessions took place after wake-up and before dopamine medication use. (E) The procedure of the EP evaluation sessions. The EP evaluation sessions contained a resting-state recording session with constant DBS (cDBS) and an evoked potential (EP) session in each hemisphere. (F) The sleep hypnogram of a sample night recording. Each 30s epoch during overnight recordings was scored into wake, REM, N1, N2, or N3 stage. (G) Power spectra of the intracranial cortical data over sensorimotor channels in REM and NREM sleep. (H) The percentage of REM and NREM during each hour segment of the overnight recordings. The percentage of REM sleep increased over the sleep course.

REM sleep predicts pathological resting-state neural signatures

During the morning resting-state recording, intracranial LFP data from BG and motor cortex were streamed in both hemispheres and the power spectra at these brain locations were evaluated. With a within-individual median split of REM duration or REM delta power, we observed that nights with longer REM duration or high REM delta power were associated with less resting beta power next morning (Figure 2A and 2B). Using LME models, we tested whether the 'duration' attributes (duration, latency) or the 'power' attributes (delta power, beta power) of REM or NREM sleep predict the morning resting-state beta power. In the 'duration' model, REM sleep duration was a negative predictor of resting beta power, $t = -2.77$, $p = .007$ (Figure 2C). Furthermore, in the 'power' model (Figure 2D), the delta power during REM sleep was also a negative predictor of resting beta power, $t = -2.27$, $p = .027$. In addition, beta power during NREM sleep was positively predicted resting beta power, $t = 2.04$, $p = .047$. Although the NREM sleep duration or delta power showed the same correlative trend as their REM counterparts in the LME models, they were not significant predictors (for results of testing NREM and REM predictors separately, see Figure 5E, 5H, and Supplementary Figure 2-5). These results suggest that longer REM sleep and stronger delta activity during REM are associated with less pathological cortical beta oscillations in the next morning.

We also calculated the phase locking value (PLV) at beta frequencies to index functional connectivity between BG and motor cortex. LME models showed that REM duration was a negative predictor of the BG-cortical PLV at beta frequencies, $t = -2.53$, $p = .014$, suggesting that longer REM sleep predicts less pathological BG-cortical hyper-functional connectivity in the next morning (Supplementary Figure 1).

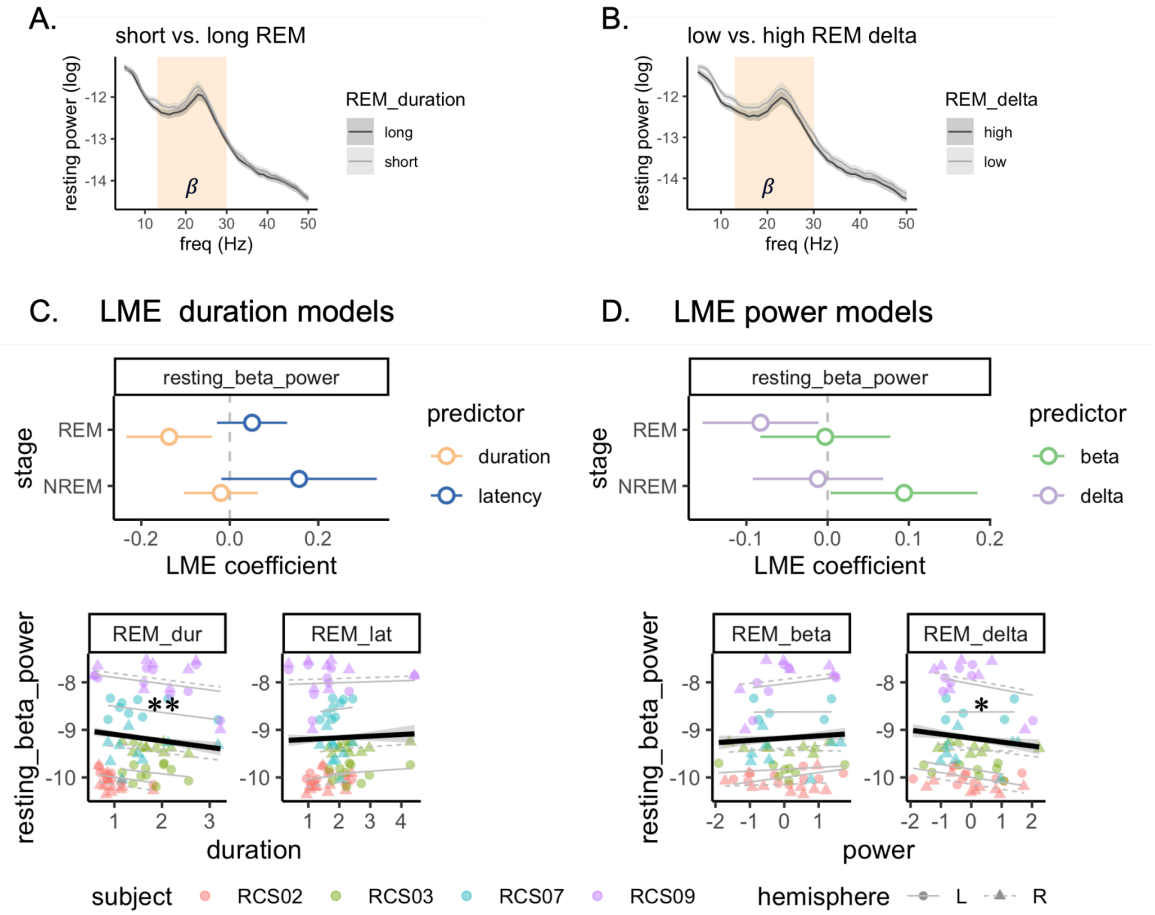

Figure 2. Sleep predicts resting-state cortical beta power. (A) The resting-state power spectrum of nights of long REM duration vs. nights of short REM duration. The highlighted area shows the frequency range of beta bands (13-30 Hz). (B) The resting-state power spectrum of nights of high REM delta power vs. nights of low REM delta power. (C) The results of linear mixed-effect (LME) models of sleep duration predictors (duration and latency) in prediction of resting-state beta power. The top panel shows the LME coefficients of duration and latency of REM and NREM sleep with 95% confidence intervals. The bottom panel shows the scatter plot of resting-state beta power against REM duration and latency. (D) The results of LME models of sleep power predictors (beta and delta) in prediction of resting-state beta power. The top panel shows the LME coefficients of delta and beta power during REM and NREM sleep with 95% confidence intervals. The bottom panel shows the scatter plot of resting-state beta power against REM beta and delta. In scatterplots, model predictions were shown at both the hemisphere level and the group level. REM_dur: REM duration; REM_lat: REM latency. Asterisks indicate statistical significance in LME models: * = p<.05, ** = p< .01.

REM sleep predicts cortico-basal effective connectivity

During the second section of the morning session, we evaluated EPs to causally assess the neural connectivity between BG and motor cortex (i.e. effective connectivity). Specifically, stimulation pulses were delivered to BG via the implanted DBS leads at a rate of 4 Hz (i.e. 250

ms per trial) while cortical field potentials were sampled at 1000 Hz. This procedure was implemented for 2 minutes in each hemisphere at a time, with the contralateral DBS off.

The evoked responses in the motor cortex consisted of an initial early response (<5 ms) which likely reflects anti-dromic activation of the hyperdirect pathway (Ashby et al., 2001; Baker et al., 2002; MacKinnon et al., 2005), and a later decaying oscillatory response (>20 ms) at primarily a beta frequency around 20 Hz which likely reflects orthodromic activation of BG projections to the cortex (Baker et al., 2002; MacKinnon et al., 2005) (Figure 3A, 3B). We assessed the amplitude and beta power of the EP to index pathophysiological hyperconnectivity in the BG-motor cortex circuit (Campbell et al., 2022). Specifically, we calculated the peak-to-peak amplitude in the initial early window (-5 to 5 ms) and the main window (20 to 100 ms), and the beta power in the whole window (-50 to 200 ms). In the 'duration' models (Figure 3C), we found that REM duration negatively and REM latency positively predicted the main-window amplitude (duration: t = -2.67, p = .009, latency: t = 2.60, p = .011) and beta power of EP (duration: t = -2.50, p = .015, latency: t = 2.17, p = .034), but not the early-window amplitude (duration: t = -0.42, p = .678, latency: t = 0.52, p = .604). In the 'power' models (Figure 3D), we found that REM delta power negatively predicted the main-window amplitude (t = -2.27, p = .028) and beta power of EP (t = -2.97, p = .004), but not the early-window amplitude (t = -0.67, p = .507). Sleep beta power, in REM or NREM, generally showed a positive trend in predicting EP metrics, but did not reach statistical significance (p's > .10). In these models which tested REM and NREM together, NREM sleep attributes were not significant predictors (for results of testing NREM and REM predictors separately, see Figure 5E, 5H, and Supplementary Figure 2-5). These results suggest that longer duration of, quicker entry into, stronger delta activity, and weaker beta activity in REM sleep predicted less pathological basal-cortical effective connectivity in the next morning.

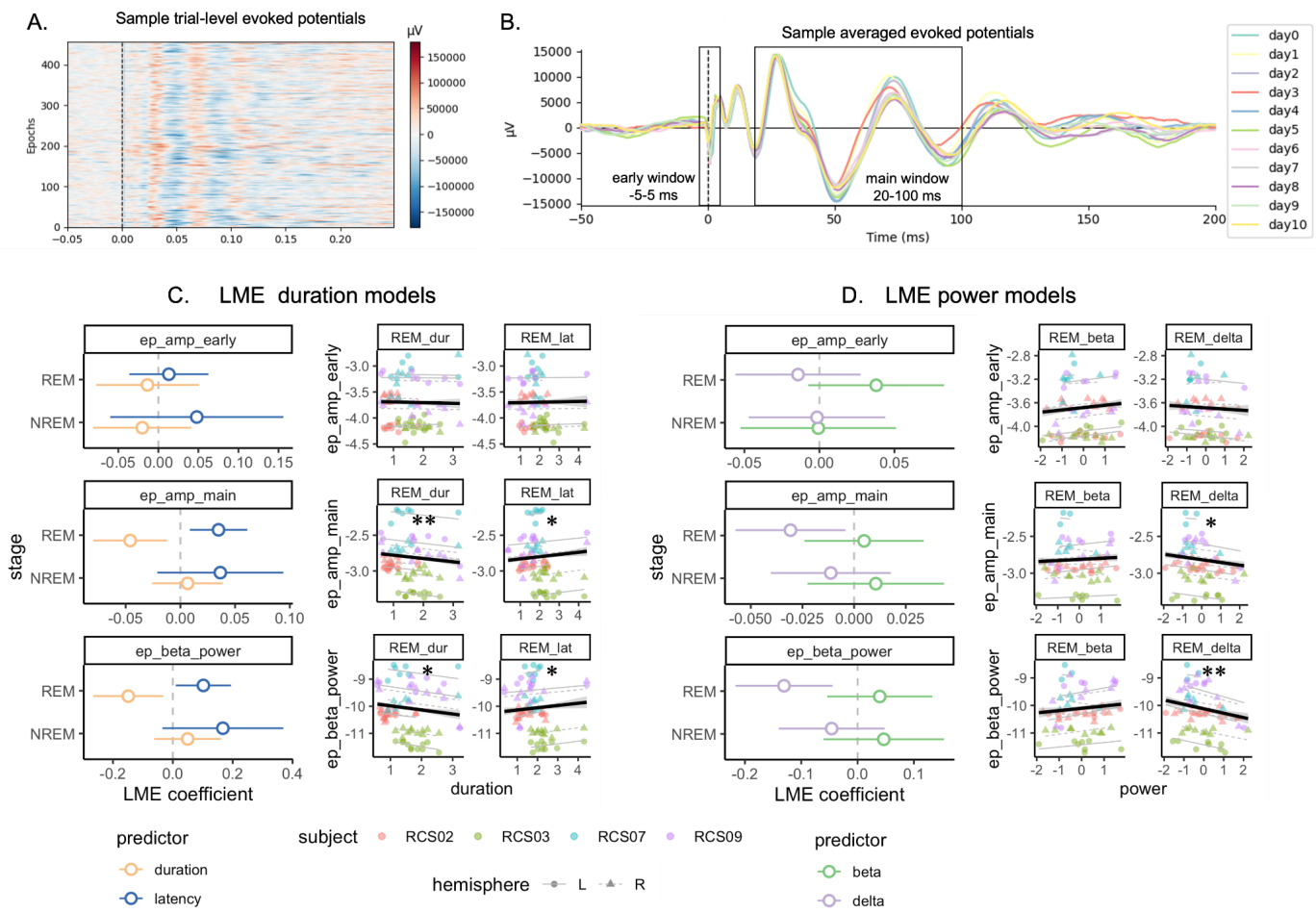

Figure 3. Sleep predicts evoked potentials (EP) in the basal ganglia-cortical circuit. (A) Trial-level cortical EP data of an example morning session. Each trial spans from -50ms to 200 ms. (B) Session-level averaged waveform of cortical EP of an example participant. At the trial level, we calculated the peak-to-trough amplitudes in an early window (-5–5 ms) and a main window (20–100 ms) and the beta power in the entire window and then averaged across trials. (C) The results of linear mixed-effect (LME) models of sleep duration predictors (duration and latency) in prediction of EP metrics. (D) The results of LME models of sleep power predictors (beta and delta) in prediction of EP metrics. In (C) and (D), the left panels show the LME coefficients with 95% confidence intervals and the right panels show the scatterplots of outcome variables against REM predictors with model predictions. ep_amp_ealry: peak-to-trough amplitude of EP in the early window; ep_amp_main: peak-to-trough amplitude of EP in the main window; ep_beta_power: beta power of the EP in the whole window; REM_dur: REM duration; REM_lat: REM latency. Asterisks indicate statistical significance in LME models: * = p<.05, ** = p< .01.

Computational modeling of evoked potentials. To further investigate the decaying oscillatory properties of EP, we modeled participants' EP data during each morning session using a damped oscillation model (Figure 4A, see Methods for details) (Eusebio et al. 2009). Across all participants, the damped oscillation model fits the EP data very well (r = 0.92 ± 0.05,

p < 1e-10) in the main time window (Figure 1B, 1C). The key parameters characterized in the damped oscillation model include initial amplitude (*Amp*), decay constant (***λ***), natural frequency (***ω***), and phase angle (***Φ***). We found that REM delta power significantly predicted 3 out 4 of these model parameters. Specifically, REM delta power was a negative predictor of initial amplitude (t = -2.42, p = .019), a negative predictor of decay constant (t = -2.10, p = .041), and a negative predictor of phase angle (t = -2.58, p = .013) (Figure 4D), suggesting that stronger REM delta activity is associated with a damped oscillatory evoked response after sleep that has a smaller amplitude and a later phase at the beginning, and decays more slowly. For the only other parameter, natural frequency, REM delta power was a marginal positive predictor (t = 1.95, p = .057). Of note, REM beta power was not a significant predictor in predicting these model parameters. Moreover, NREM delta and beta did not predict any of these model parameters. These results may imply that delta activity during REM sleep plays a significant role in the overnight neural plasticity of the BG-cortex circuit.

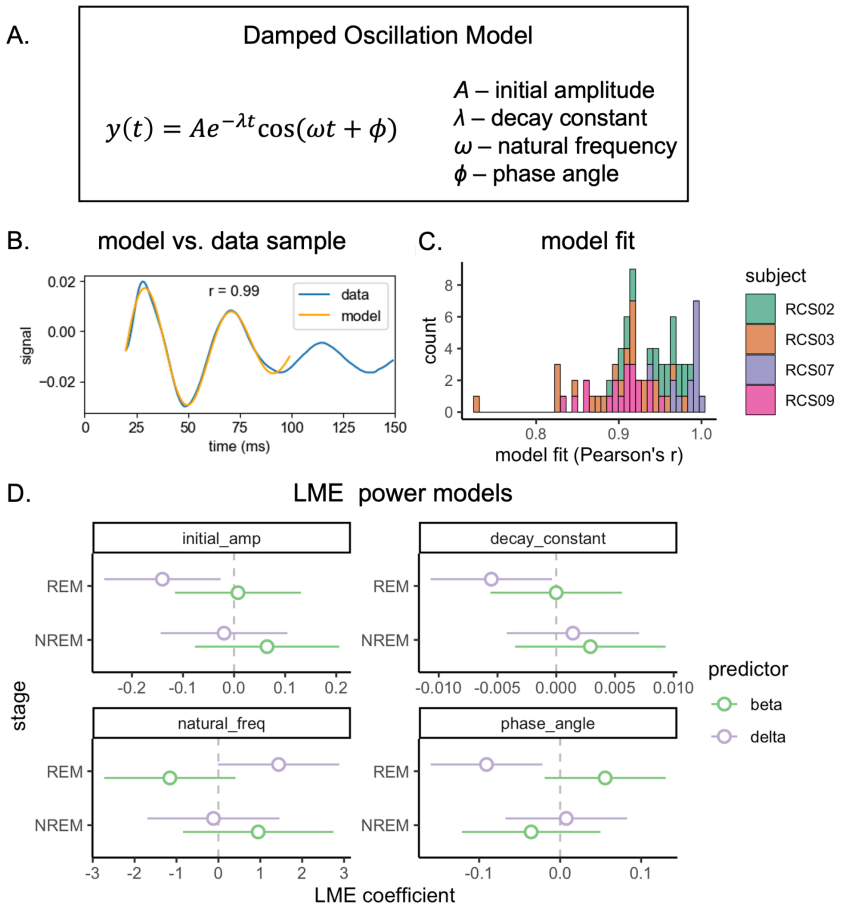

Figure 4. Damped oscillation modeling of evoked potentials. (A) The damped oscillation model with four major parameters: initial amplitude, decay constant, natural frequency, and phase angle. (B) Actual vs. modeled EP waveform in the main window of an example session. (C) Distribution of model fit across participants. (D) Results of LME models of sleep beta and delta power in prediction of the major parameters of the damped oscillation modeled EP waveform.

Detection of delta waves and beta bursts during sleep

Given the importance of sleep delta activity shown above, we further evaluated individual delta waves during sleep. As the metric of delta power naturally takes into consideration both the amplitude and frequency of the occurrence of delta waves, we analyzed their amplitude and occurrence rate separately and compared them with delta power. Following prior research (Bernardi et al. 2019), we detected delta half-waves in the cortex during sleep using an algorithm of analyzing consecutive zero-crossings. The detected delta waves were present in both REM and NREM sleep stages, with greater rate of occurrence in NREM (N3 and N2) than REM (Figure 5C). Their raw waveform showed a “sawtooth” shape and their average waveform showed a non-sinusoidal sharp peak (Figure 5A, 5B). As expected, the peak amplitude of delta waves was larger in N3 (i.e. slow-wave sleep) than REM sleep (Figure 5D). We further tested in separate LME models whether the peak amplitude or occurrence rate of these delta bursts predict next-morning pathological neural signatures. In both REM and NREM sleep, compared to overall delta power, peak amplitude of delta bursts had greater or comparable standardized coefficients (z-stat) while their occurrence rate generally had smaller standardized coefficients (Figure 5E), underscoring the importance of the peak amplitude of these delta waves. Compared to N3 and N2, the peak amplitude of REM delta waves had greater standardized coefficients, highlighting the role of REM delta waves.

Results above showed that sleep beta power was a numerically positive predictor of morning pathological neural signals. For comparison, we also detected beta bursts during sleep and calculated their amplitude and occurrence rate. We found that beta bursts had a higher occurrence rate and a greater amplitude in REM than in N3 (Figure 5F, 5G). When tested in separate LME models to predict morning pathological neural signatures (Figure 5H), in contrast to our delta findings, beta burst occurrence rate had greater standardized coefficients than overall beta power while the beta burst amplitude showed a lower coefficient, highlighting the uniquely pathological role of beta bursting rate during sleep.

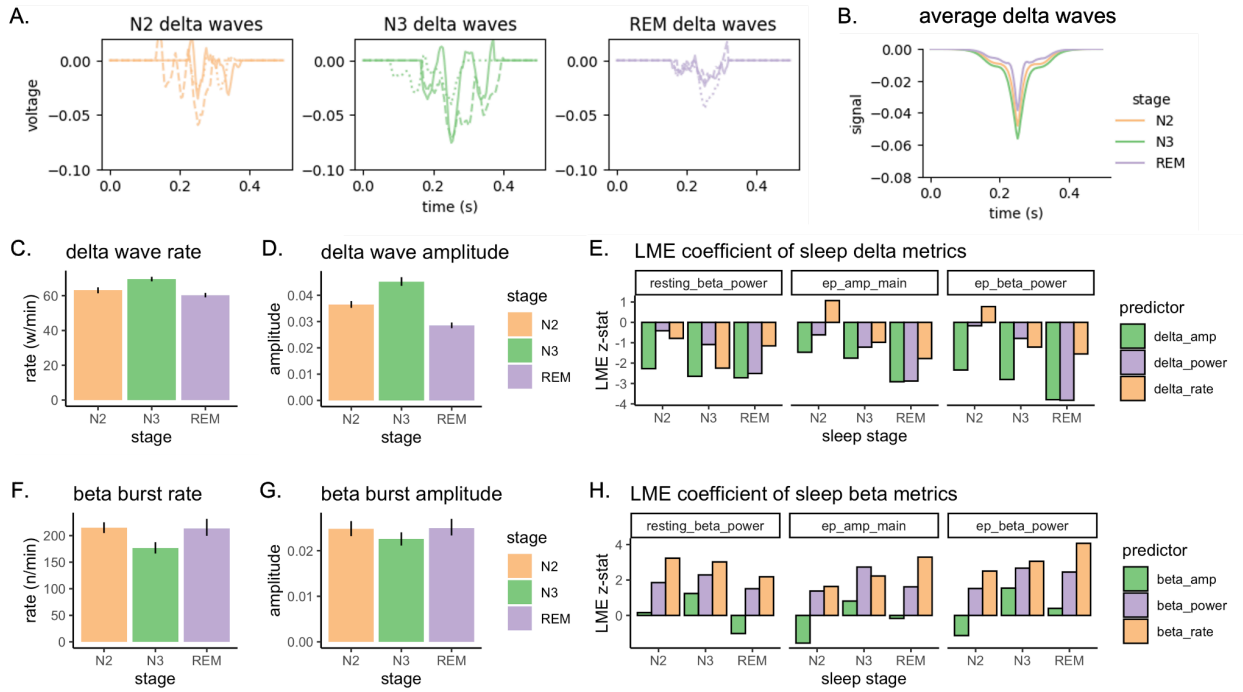

Figure 5. Detection of delta waves during sleep. Sample negative delta half-waves are shown for N2, N3, and REM stages at both individual (A) and averaged (B) levels. The individual delta half-waves were aligned at their negative peak and averaged accordingly. (C) and (D) Occurrence rate and amplitude of detected delta waves across sleep stages. (E) Standardized LME coefficients of delta wave metrics across sleep stages in prediction of morning pathological neural signatures. (F) and (G) Occurrence rate and amplitude of beta bursts across sleep stages. (E) Standardized LME coefficients of beta metrics across sleep stages in prediction of morning pathological neural signatures.

Timing effect of REM sleep

Our analyses above showed a critical role of REM sleep in the pathological BG-cortical circuit in PD. One question is whether this protective role is influenced by the temporal structure of NREM and REM sleep. To answer this question, we calculated the relative proportion of time spent in NREM versus REM sleep (Figure 1H) and the delta power in NREM versus REM throughout the sleep course (Figure 6A). Along with the percentage of REM sleep, the delta power during REM sleep also increased moderately over the sleep course, $t = 2.42$, $p = .019$ (Figure 6B). In order to test the role of REM and NREM sleep individually, we tested their effects in prediction of next-morning pathological neural signatures in separate LME models for each hour segment.

The delta power during early REM sleep was a null predictor of the effective connectivity indices (main-window amplitude and beta power of EP). However, the predictive effect of REM delta grew stronger and became a significant negative predictor for later hours (Figure 6C). NREM delta power, in contrast, remained a null or a less strong negative predictor and did not show a clear temporal trajectory throughout the course of sleep. Furthermore, REM percentage

was a significant negative predictor of morning pathological neural signatures only during late hours and remained null during early hours (Figure 6D). NREM percentage, in contrast, was a null predictor during most hours and could be a positive predictor during either early or late hours. These results suggest a timing effect of the protective role of REM sleep (its length and delta activity) in maintaining a healthy profile of BG-cortical circuit. The effect of REM sleep was more pronounced during the later hours of sleep.

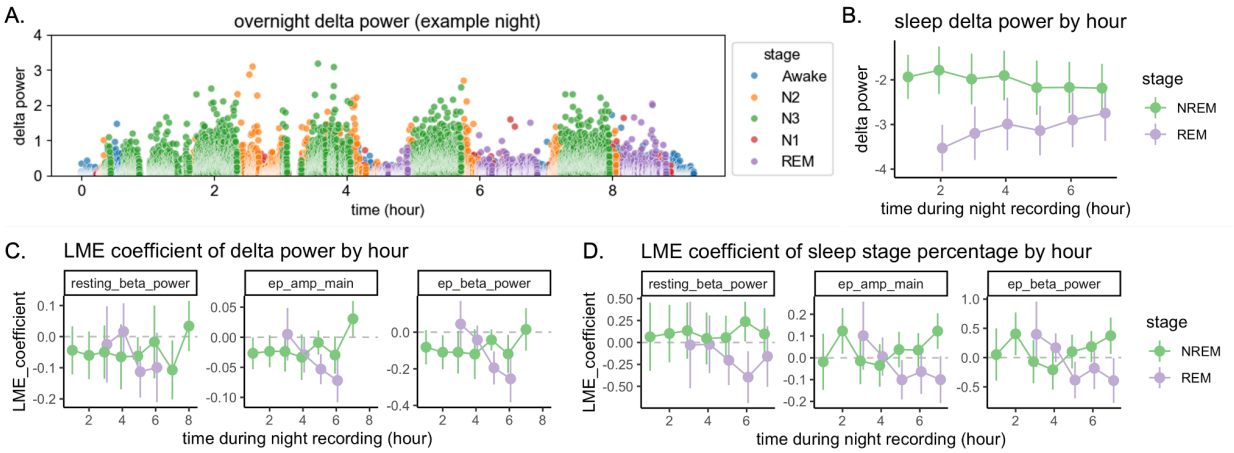

Figure 6. Timing effect of REM sleep over the sleep course. (A) Delta power over the sleep course of an example night. (B) Average delta power in REM and NREM sleep during each hour segment over the sleep course across participants. (C) LME coefficients of REM and NREM delta power by each hour segment in prediction of morning pathological neural signatures. Predicting resting beta power: REM delta was a negative predictor at hour 5 (t = -2.68, p = .011), and NREM delta was a negative predictor at hour 7 (t = -2.22, p = .038). Predicting EP amplitude in the main window: REM delta was a negative predictor at hour 5 (t = -4.18, p < .001) and hour 6 (t = -3.89, p < .001), and NREM delta was not a significant predictor at any hour. Predicting EP beta power: REM delta was a negative predictor at hour 5 (t = -4.25, p < .001) and hour 6 (t = -3.89, p < .001), and NREM delta was a negative predictor at hour 2 (t = -2.32, p = .025) and hour 6 (t = -2.24, p = .035). All other LME tests were non-significant, p's >.05. (D) LME coefficients of REM and NREM duration percentage by each hour segment in prediction of morning pathological neural signatures. Predicting resting beta power: REM percentage was a negative predictor at hour 6 (t = -2.63, p = .011), and NREM percentage was a positive predictor at hour 6 (t = 2.06, p = .044). Predicting EP amplitude in the main window: REM percentage was a negative predictor at hour 5 (t = -2.19, p = .032), and NREM percentage was a positive predictor at hour 2 (t = 2.31, p = .024) and hour 7 (t = 2.97, p = .004). Predicting EP beta power: REM percentage was a negative predictor at hour 5 (t = -2.41, p = .019) and hour 7 (t = -2.01, p = .049), and NREM percentage was a positive predictor at hour 2 (t = 2.17, p = .033) and hour 7 (t = 2.36, p = .022). All other LME tests were non-significant, p's >.05. Error bars indicated 95% confidence intervals.

Discussion

In this study, we followed the sleep of 4 PD patients for multiple nights and subsequent mornings while recording intracranially from the motor cortex and the basal ganglia. We assessed the pathological neural signatures of PD patients, including resting-state beta oscillation, and functional and effective BG-cortical connectivity. We showed that longer REM sleep duration and shorter REM sleep latency predicted reduced pathological neural signatures. When looking within REM sleep, we found that delta power in the cortex predicted reduced pathological neural signatures, while beta power, in some cases, predicted increased pathological neural signatures. We further detected individual delta waves during NREM and REM sleep using an established algorithm. We confirmed that the amplitude of these delta waves predicted reduced pathological neural signatures, with stronger prediction from REM delta waves than from NREM delta waves. In contrast, the amplitude of beta bursts during REM and NREM sleep predicted increased pathological neural signatures. Also, the protective effects of REM sleep grew stronger as REM sleep accumulated across the night. In contrast, the effect of NREM sleep was relatively steady and less pronounced than REM sleep throughout the night.

Protective role of delta activity during sleep

Our results suggest a protective role of slow-wave delta activity during sleep in relation to daytime pathological neural network activity in PD. In REM sleep, delta activity predicts less resting beta oscillation and less hyper-effective connectivity between BG and motor cortex, which are neuropathological hallmarks of PD (Brown 2003). This is consistent with findings that slow wave activity during sleep is beneficial in several ways in neurodegeneration diseases, including PD (Schreiner et al. 2019; J. Chen et al. 2024) and AD (Wunderlin et al. 2020; Lee et al. 2020; Ju et al. 2017). It is worth noting that this effect of delta was not driven by the inverse relationship between delta and beta activity during sleep (Anjum et al. 2024). Beta activity during sleep was numerically predictive of increased pathological neural signatures next morning but this effect was less strong than the effect of sleep delta activity, especially when they were tested together (Figure 2D, 3D, 4D). This suggests that during sleep, slow-wave delta activity, rather than beta activity, plays a central role in attenuating the pathological neural activity in PD.

Sleep and neural plasticity

We employed evoked potentials to assess the effective connectivity between basal ganglia and the motor cortex. Computational modeling of the evoked potential as a damped oscillation yielded very good fits. Interestingly, we found that several characteristics of the decaying oscillation model were predicted by REM delta activity. These characteristics include not only the initial amplitude of the evoked response, but also how fast it decays (decaying constant), how frequent it oscillates naturally (natural frequency), and at what phase angle the oscillation starts (starting phase angle). These oscillatory characteristics of evoked potentials are thought to reflect the intrinsic network architecture and their changes suggest neural plasticity. Our finding of REM delta predicting changes in those characteristics suggests the existence of REM sleep-related neural plasticity in the BG-cortical network, especially during the occurrence of delta activity. This is consistent with animal research findings that REM sleep promotes neural plasticity (Aime et al. 2022; Dumoulin Bridi et al. 2015).

REM vs. NREM sleep in relation to neurodegeneration

It is notable that REM sleep is more strongly related to next-morning pathological neural signatures than NREM sleep. In our LME models, several REM parameters (e.g., longer duration, shorter onset latency, stronger delta activity, and less beta activity) significantly predicted less next-morning pathological neural signals but their NREM counterparts were not a significant predictor. Although abnormalities in REM sleep (i.e., REM sleep behavior disorder) are a strong precursor of PD (Schenck, Boeve, and Mahowald 2013), most prior studies in this field have focused on NREM sleep when researching PD (Schreiner et al. 2019; J. Chen et al. 2024). It is worth noting that when tested separately, the coefficients of NREM and REM delta activities have the same negative sign (Figure 5E), and when tested together, the coefficient of NREM delta activity became closer to zero while that of REM delta activity remained significant (Figure 2D and 3D). This suggests that NREM delta activity is likely to be beneficial in reducing wakeful neural malfunctioning in PD, which is consistent with prior research on NREM sleep and neurodegeneration (Schreiner et al. 2019; J. Chen et al. 2024), although not as strongly as REM delta activity, at least in the outcome measures we tested. Beyond the existing literature, our results underscore the importance of REM sleep regarding the neural health of PD in particular and neurodegenerative diseases in general.

Furthermore, we found that the effect of REM delta activity was not constant throughout the night. Instead, its effect started from nearly zero in the middle of the sleep course and got increasingly strong as sleep progressed (Figure 6C). This is congruent with the fact that as the night progressed, REM sleep became more prevalent (Figure 1H) and the delta activity during REM sleep also increased in strength (Figure 6B). This suggests a timing effect of REM sleep and its delta activity: REM delta activity becomes increasingly beneficial as sleep progresses, possibly due to a cumulative effect. This could also simply be a by-product of the increased REM delta power in later hours: REM delta activity matters more when it is stronger. Nevertheless, we show that despite generally stronger delta activity during NREM sleep than REM sleep throughout the night, the effect of NREM delta activity was generally insignificant and held stable over the sleep course. Our finding of this timing effect of REM sleep may have implications for PD patients who experience early awakenings in the morning.

Delta activity during REM sleep

Beyond calculating delta power, we further detected positive and negative half-waves of the delta frequency in the sensorimotor cortical channel during nighttime recordings. Consistent with prior research (Bernardi et al. 2019), we identified delta half-waves in both NREM and REM stages. We show that they generally have a triangular shape and their peak amplitude was greater during N3 than REM sleep. Interestingly, the peak amplitude of these delta half-waves was a much stronger negative predictor of next-morning neural signatures than FFT-calculated delta power. This suggests that the appearance of these delta waves may be a more direct benefiting factor for neural functioning in PD.

Consistent with analyses with delta power, we show that the standardized coefficient of the delta half-waves was larger in REM sleep compared to NREM stages, underscoring the

unique role of REM delta waves. Using EEG, prior research has shown that the “sawtooth” delta waves during REM sleep have a medial M1 source, matching the position of our ECoG electrodes. Unlike typical slow waves during N3, “sawtooth waves” in REM tend to be associated with increased eye movements and gamma activity, suggesting increased neuronal firing (Bernardi et al. 2019; Steriade, Amzica, and Contreras 1996). It is possible that REM-specific “sawtooth waves”, together with associated activities, play an important role in regulating the BG-cortical circuit in PD.

Concluding remarks

By following a group of PD patients for multiple nights, we show that REM sleep predicts less neural network malfunctioning the next morning. Specifically, we assessed several established pathological neural signals in PD in the BG-cortical circuit following at-home sleep. We found that the delta activity during REM sleep plays a central role in this protective effect. Our findings highlight a potentially unique role of REM sleep in the progression of Parkinson’s diseases. Future research is needed to further examine the role of REM sleep in other neurodegenerative diseases or other aspects of disease progression.

Methods

Participants

The study was registered on clinicaltrials.gov (NCT0358289; IDE G180097), and the study protocol was approved by the Institutional Review Board. The four participants presented in this study were diagnosed with idiopathic Parkinson's disease (Supplementary Table 1), and were enrolled as part of a parent study investigating adaptive deep brain stimulation protocols (Gilron et al. 2021; Oehrn et al. 2024).

Participants were implanted with bilateral quadripolar electrodes capable of both sensing and stimulation. RCS02 and 07 received these electrodes in the Subthalamic Nucleus (STN) using Medtronic model 3389 leads, and RCS03 and 09 were implanted in the Globus Pallidus (GP) with Medtronic model 3387 leads. The selection of the implant site was determined by the clinical team of each participant. Subdural quadripolar electrocorticogram (ECoG) arrays (Medtronic Resume II, model 0913025) were implanted bilaterally over the central sulcus. All electrodes were connected to Summit RC+S (Medtronic model B35300R) implantable neural stimulators (INS), which have been extensively described in previous studies (Smyth et al. 2023; Anjum et al. 2024; Gilron et al. 2021). The Summit RC+S system enables the recording of field potentials from both cortical and basal ganglia locations during chronic stimulation. It also allows for the streaming of data recordings to a nearby tablet for offline analysis while the participant is at home.

Subject Demographics and Clinical Information				
	RCS02	RCS03	RCS07	RCS09
Demography				
Age	58	66	40	48
Gender	M	M	M	M
Diagnosis	PD	PD	PD	PD
Duration (Years)	11	13	9	13
DBS stimulation settings				
Stim target	STN	GP	STN	GP
Pulse width (μs)	60	60	60/90	90
Stim amp. (mA)	L: 2.4 R: 3.1	L: 3.7 R: 2.8	L: 1.7–3.4 R: 1.7–3.4	L: 3–3.7 R: 3–3.7
Stim freq. (Hz)	130.2	178.6	130.2	150.6
Stim contact	L: C+2– R: C+1–	L: C+1– R: C+1–	L: C+2– R: C+2–	L: C+2– R: C+2–
Symptoms and clinical characteristics				
Medication details	C-Ldopa 25–100 mg IR (3 times daily) Aman-H 100 mg (3 times daily)	C-Ldopa 25–100mg CR (1–2 tabs at bedtime) and 25–100 mg IR (3 times daily)	C-Ldopa 25–100mg (1 time daily) Rasagiline (Azilect) 1mg (1 time daily)	Rytary 195mg (3 times daily)
UPDRS-III (OFF)	49	66	41	39
UPDRS-III (ON)	5	24	14	16
UPDRS 1.7	No sleep symptoms	Slight sleep symptoms	Slight sleep symptoms	Mild sleep symptoms
UPDRS 1.8	No daytime sleepiness	Mild daytime sleepiness	Moderate daytime sleepiness	Mild daytime sleepiness
Sleep diagnosis	No sleep conditions	Nocturia; RBD	Daytime sleepiness	OSA; Insomnia
Neuropsych report (pre-op)	No reported sleep disorder or conditions	Mild sleep difficulties with nocturia and RBD	Day time sleepiness	Had long-term difficulties sleeping before PD.
Total Hours Recorded				
Left Device	60.3	68.4	42.9	47.1
Right Device	57.0	45.3	48.0	41.3

Supplementary Table 1 - Subject Information. *C-Ldopa: Carboxy-Levodopa. Aman-H: Amantadine-Hydrochloride. RBD: REM-sleep Behavior Disorder. OSA: Obstructive Sleep Apnea. UPDRS: Unified Parkinson's Disease Rating Scale (obtained prior to DBS implantation)*

Experimental procedures

Participants maintained their typical sleep schedule at home for approximately 10 nights (Supplementary Table 1), most of which were consecutive. Overnight sleep at home was recorded concurrently using portable PSG with the DREEM2 headset, alongside intracranial cortico-basal data streaming via the RC+S system. After awakening and before medication use, participants had a morning session that included 1-minute resting-state recording and 4-minute evoked potential recording (2 minutes each hemisphere). Only intracranial data were recorded in the morning sessions. All data recordings were conducted remotely in the participants' homes. All participants continued their regular dopaminergic medication throughout the study. During sleep and resting-state recording, participants received their clinical continuous DBS

therapy and regular medications. We initially collected a total of 42 night+morning pairs of data. The EP data of 3 morning sessions of RCS07 failed to be recorded and were thus excluded. Valid data of a total of 39 night+morning pairs were used for analysis.

Overnight data acquisition

The DREEM2 headband collects electroencephalography (EEG) data and autonomic signals including pulse oximetry, electromyography, and accelerometry. The DREEM2 headband provided sleep stage classification hypnograms according to AASM scoring methods with an automated sleep staging algorithm. The accuracy of these automatic sleep stage labels is comparable to that provided by certified experts (Arnal et al. 2020). This has also been previously validated as matching expected intracranial neurophysiology in PD by our group in a separate study focused on NREM sleep (Anjum et al. 2024).

Three intracranial field potential streams were recorded at a sampling rate of 500 Hz. The basal ganglia potentials were measured using a bipolar 'sandwich' electrode configuration that captures the electric potential difference between two electrodes adjacent to the stimulation electrode. Cortical field potentials were recorded in two streams: one using a bipolar configuration on the precentral gyrus and another bipolar configuration spanning the entire electrode array across the central sulcus. Participants recorded about ten nights of both external polysomnogram and intracranial field potential data during ongoing therapeutic stimulation.

Data alignment involved correlating sleep stages from the polysomnogram with intracranial field potentials. To address discrepancies in sampling rates and time offsets between the DREEM and RC+S data streams, cross-correlation analysis was employed on the accelerometry data from each device, adjusting the temporal alignment to maximize correlation, as detailed in our previous report (Anjum et al. 2024). The resulting dataset includes a sleep stage label (N1, N2, N3, REM, Wake) for each 30-second epoch of the intracranial field potential streams for each hemisphere.

Morning data acquisition

During resting-state morning recording, intracranial data were streamed with the same setting as the overnight recording. During the evoked potential procedure, stimulation pulses were delivered in each hemisphere at the basal ganglia stimulation electrode at a rate of 4 Hz, with an amplitude of 4 mA, and with the same pulse width as their clinical stimulation (60 or 90 μs). Field potentials were recorded at a sampling rate of 1000 Hz from one cortical electrode and one subcortical electrode ipsilaterally. This procedure was implemented for 2 minutes in each hemisphere at a time, with the contralateral DBS off (e.g. left device for 2 minutes with right device off, then vice versa).

Overnight intracranial data analysis

Power spectrum analysis – Power spectra were calculated in 2-second windows for each participant and each sleep stage via Welch's technique using the scipy python package, with a Hann window, 1000-point segments (2s sample), and 0 overlap between segments. Delta power was the sum of power from 0.5-4 Hz and beta power was the sum of power from 13.5-30 Hz. Both delta and beta powers were log-transformed and then z-scored within each channel of each hemisphere for statistical tests.

Detection of delta waves – From the intracranial cortical data during overnight sleep recordings, we detected delta waves using a previously established method (Bernardi et al. 2019; Riedner et al. 2007). Specifically, the signal of each cortical channel was first down-sampled to 125 Hz and bandpass filtered between 1 and 10 Hz (the upper limit of the filter was selected to minimize wave shape and amplitude distortions). An algorithm based on detecting consecutive signal zero-crossings (Bernardi et al. 2019; Riedner et al. 2007) was used to detect delta waves during sleep. Negative half-waves with a duration of consecutive zero-crossings between 125 and 500 ms (1– 4 Hz) were extracted, and the following properties were quantified: peak amplitude (mV, in absolute value) and duration (ms). The average peak amplitude and occurrence rate were quantified in each sleep stage. Raw signal before down-samping and filtering corresponding to the detected negative half-waves was used for delta wave visualization (Figure 5A).

Detection of beta bursts – The intracranial cortical data were first down-sampled to 250 Hz and bandpass filtered in the beta frequency range (13-30 Hz). The amplitude envelope was calculated on the preprocessed data using a Hilbert transform ('hilbert' from scipy). For each channel across all the nights of a participant, the 75 percentile of the beta amplitude envelope was set as the threshold of a beta burst, following prior research (Tinkhauser, Pogosyan, Tan, et al. 2017; Tinkhauser, Pogosyan, Little, et al. 2017). Beta bursts were detected as the amplitude envelope exceeding the threshold, and their average peak amplitude and occurrence rate were calculated in each sleep stage.

Morning resting-state data analysis

Intracranial data of all channels in both hemispheres during the resting-state recording (1 min) were extracted for each morning session. The power spectral density was calculated for the extracted data using Welch's method ("psd_array_welch" in MNE time-frequency) with a Hamming window, 500-point segments (1s sample), and 0 overlap to avoid over-sampling of middle segments during this short recording. Beta band power was calculated as the sum of power from 13-30 Hz and further log-transformed for later analyses.

The BG-cotical functional connectivity was quantified as the phase locking value (PLV) between the basal ganglia channel and the cortical channels in the extracted resting-state data, with a "cwt_morlet" time-frequency decomposition method and a hanning smoothing kernal ("spectral_connectivity_time" in MNE_connectivity). PLV at the beta frequency was extracted and averaged.

Evoked potential data analysis

Intracranial data of subcortical and cortical channels during the evoked potential recording were extracted for each trial into 250-ms epochs ("mne.EpochsArray") with 50ms pre-stimulation baseline. For each recording session, the data of beginning 10s and ending 2s were excluded from analyses because of signal disruption due to changes of stimulation frequency and amplitude. Each trial's data were baseline corrected and trials were rejected if the amplitude in the cortical channel exceeded 0.2 V or in the subcortical channel exceeded 1 V. Temporally misaligned trials due to packet loss in the RC+S system were visually inspected and rejected. After preprocessing, each hemisphere retained an average of 491 (SD=146,

median=468) trials in a session (see Figure 2A and 2B for example plot of trial-level and session-level EP respectively).

For each EP trial of the cortical channel data, we calculated the peak-to-trough amplitudes in an early window (-5 to 5 ms) and a main window (20 to 100 ms) and the power spectral density of the whole epoch using Welch's method ("psd_array_welch" in MNE time-frequency). These trial-level EP metrics were averaged for each hemisphere and each session.

Damped oscillation modeling

In order to understand other characteristics of EP, we further analyzed the main window of EP (20 to 100 ms) using damped oscillation modeling (Eusebio et al. 2009). An average waveform of EP was calculated for each hemisphere per each session. The main window data were fit with a decaying cosine function of time (*t*):

$$y(t) = Ae^{-\lambda t} cos(\omega t + \phi) + kt + b$$

Where A is the initial amplitude when $t=0$, λ is the decaying constant, ω is the oscillatory angle frequency, ϕ is the starting phase angle, and $kt + b$ is a drifting baseline with time. The model was fitted to the data with optimization method "curve_fit" from the scipy python package that optimizes for least squares of error. We used the Pearson's r between the predicted and actual data as the model fit metric (Figure 4C).

Statistical tests

We used Linear Mixed-Effects (LME) Models to test the effects of sleep parameters on next-morning pathological neural signatures in R, with "lmer" function from "lme4" and "lmerTest" package. In the main analyses, we include both REM and NREM parameters in the same model as the fixed effects, and participant and hemisphere as nested random effects. Specifically, we tested the effects of REM and NREM sleep duration or latency together in the "duration" models. We tested the effects of beta and delta power in REM and NREM together in the "power" models. In the secondary analyses testing the effects of delta power and sleep stage percentage over time, we tested the effects of individual predictors in separate LME models and obtained their model coefficients with 95% confidence intervals. In the secondary analyses of testing the effects of delta power vs. delta wave metrics and beta power vs. beta burst metrics, we tested the effects of individual predictors in separate LME models and obtained their standardized statistics (z-stat) because the predictors are on different scales.

Supplementary Materials

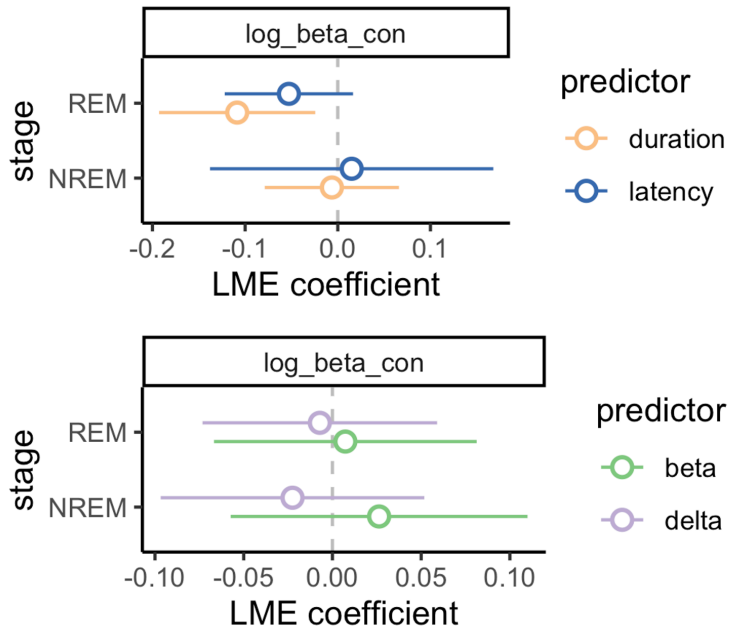

Supplementary Figure 1. The results of linear mixed-effect (LME) models of sleep predictors in prediction of resting-state BG-cortical functional connectivity at beta frequencies. Error bars indicate 95% confidence intervals of LME coefficient.

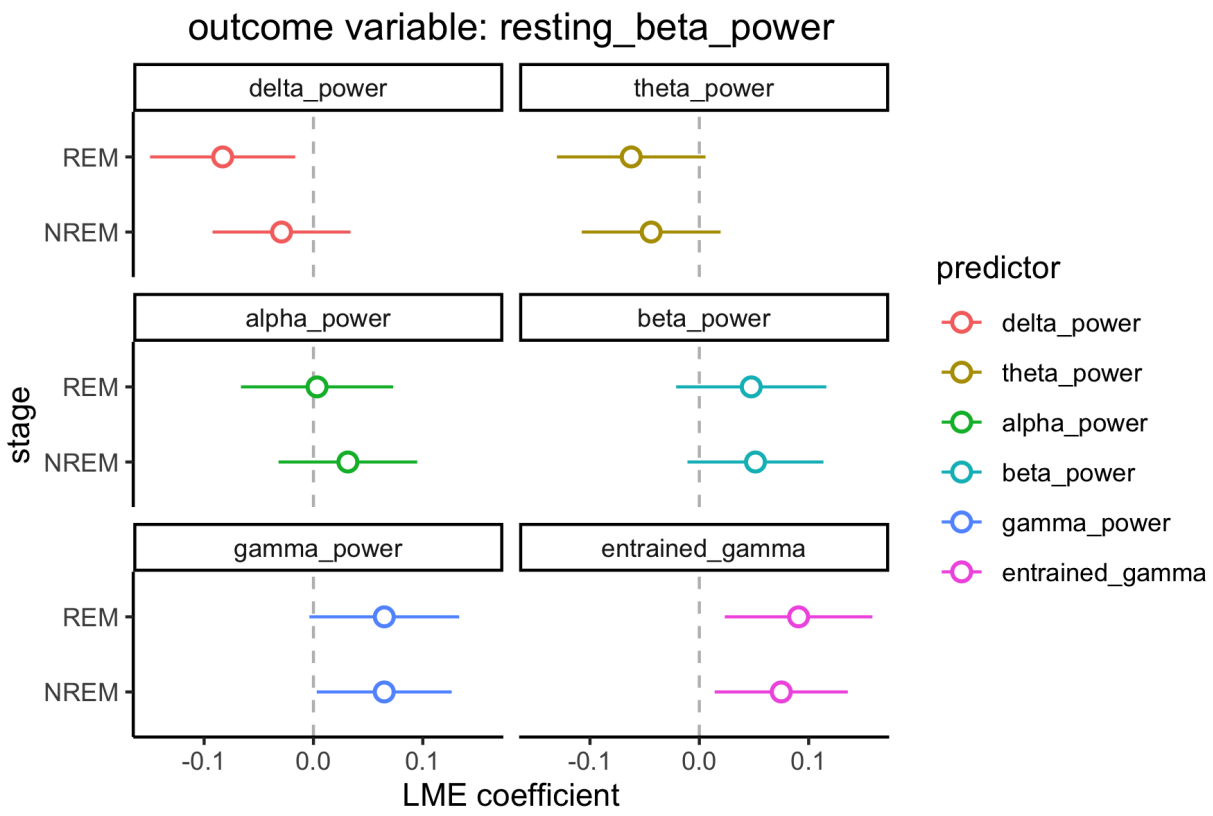

Supplementary Figure 2. The results of linear mixed-effect (LME) models of various power predictors in prediction of resting-state beta power. The power predictors include delta power (1-4 Hz), theta power (4-8 Hz), alpha power (8-13 Hz), beta power (13-30 Hz), gamma power (30-60 Hz), and entrained gamma power (±2 Hz around patients' half-stimulation frequency). Each of these power predictors was tested in individual LME models separately, and also separately for REM and NREM power. Error bars indicate 95% confidence intervals of LME coefficient.

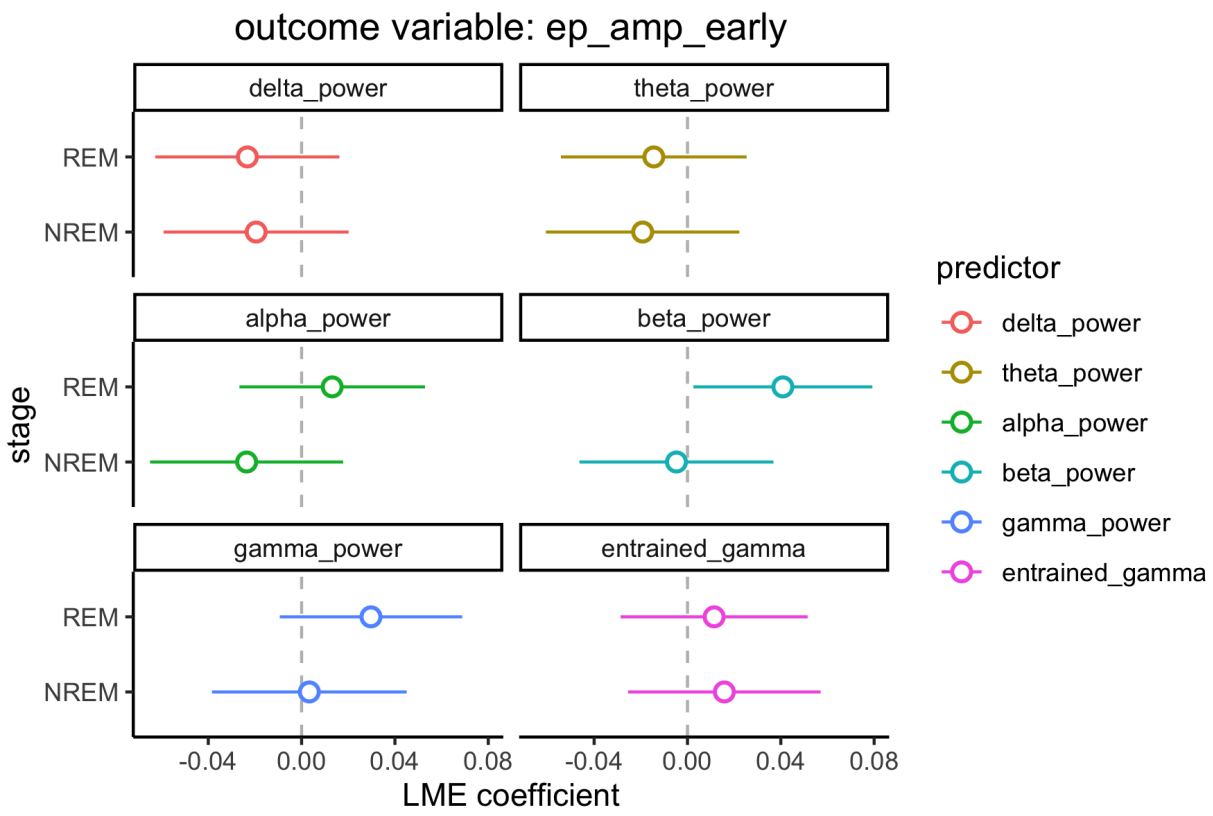

Supplementary Figure 3. The results of linear mixed-effect (LME) models of various power predictors in prediction of amplitude of evoked potentials (EP) in the early window. The power predictors include delta power (1-4 Hz), theta power (4-8 Hz), alpha power (8-13 Hz), beta power (13-30 Hz), gamma power (30-60 Hz), and entrained gamma power (±2 Hz around patients' half-stimulation frequency). Each of these power predictors was tested in individual LME models separately, and also separately for REM and NREM power. Error bars indicate 95% confidence intervals of LME coefficient.

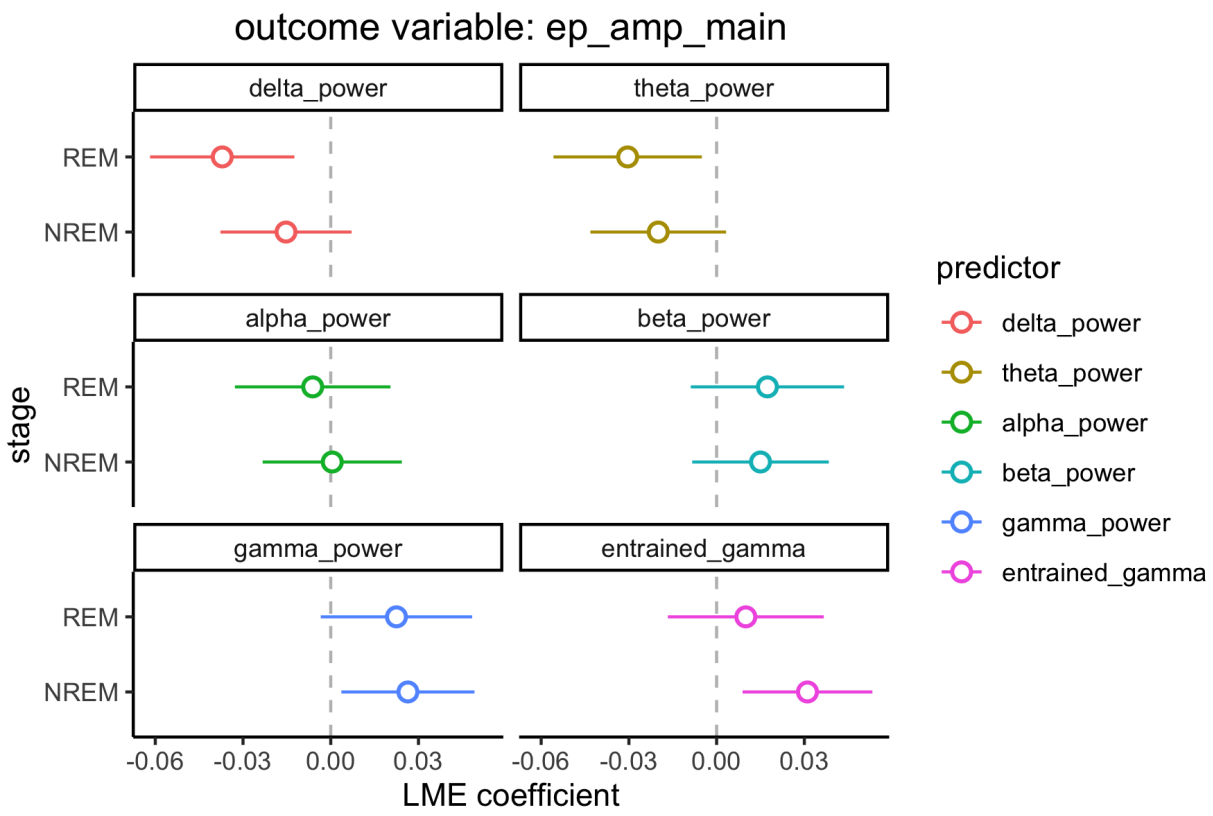

Supplementary Figure 4. The results of linear mixed-effect (LME) models of various power predictors in prediction of amplitude of evoked potentials (EP) in the main window. The power predictors include delta power (1-4 Hz), theta power (4-8 Hz), alpha power (8-13 Hz), beta power (13-30 Hz), gamma power (30-60 Hz), and entrained gamma power (±2 Hz around patients' half-stimulation frequency). Each of these power predictors was tested in individual LME models separately, and also separately for REM and NREM power. Error bars indicate 95% confidence intervals of LME coefficient.

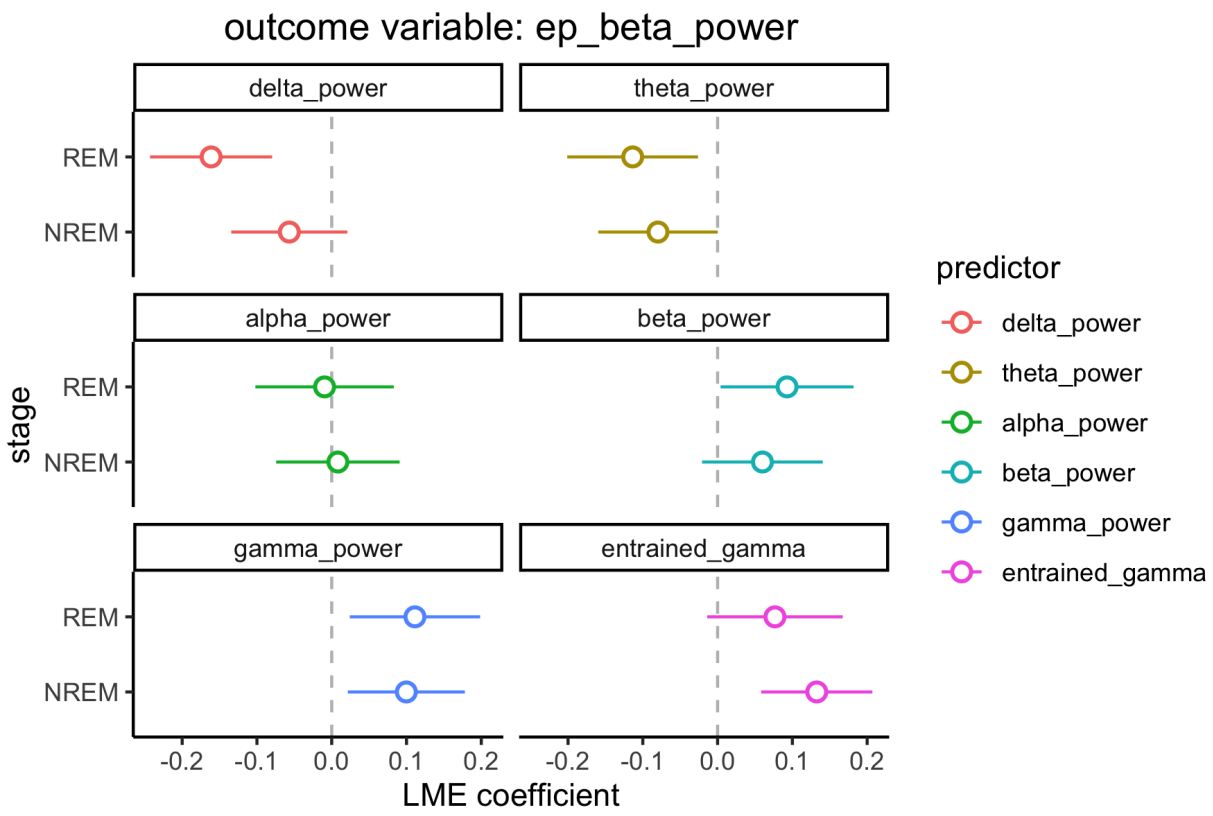

Supplementary Figure 5. The results of linear mixed-effect (LME) models of various power predictors in prediction of the beta power of evoked potentials (EP). The power predictors include delta power (1-4 Hz), theta power (4-8 Hz), alpha power (8-13 Hz), beta power (13-30 Hz), gamma power (30-60 Hz), and entrained gamma power (±2 Hz around patients' half-stimulation frequency). Each of these power predictors was tested in individual LME models separately, and also separately for REM and NREM power. Error bars indicate 95% confidence intervals of LME coefficient.

References

Aime, Mattia, Niccolò Calcini, Micaela Borsa, Tiago Campelo, Thomas Rusterholz, Andrea Sattin, Tommaso Fellin, and Antoine Adamantidis. 2022. “Paradoxical Somatodendritic Decoupling Supports Cortical Plasticity during REM Sleep.” *Science (New York, N.Y.)* 376 (6594): 724–30.

Anjum, Md Fahim, Clay Smyth, Rafael Zuzuárregui, Derk Jan Dijk, Philip A. Starr, Timothy Denison, and Simon Little. 2024. “Multi-Night Cortico-Basal Recordings Reveal Mechanisms of NREM Slow-Wave Suppression and Spontaneous Awakenings in Parkinson’s Disease.” *Nature Communications* 15 (1): 1793.

Arnal, Pierrick J., Valentin Thorey, Eden Debellemaniere, Michael E. Ballard, Albert Bou Hernandez, Antoine Guillot, Hugo Jourde, et al. 2020. “The Dreem Headband Compared to Polysomnography for Electroencephalographic Signal Acquisition and Sleep Staging.” *Sleep* 43 (11): zsaa097.

Bernardi, Giulio, Monica Betta, Emiliano Ricciardi, Pietro Pietrini, Giulio Tononi, and Francesca Siclari. 2019. “Regional Delta Waves in Human Rapid Eye Movement Sleep.” *The Journal of Neuroscience: The Official Journal of the Society for Neuroscience* 39 (14): 2686–97.

Berry, R. B., R. Brooks, C. E. Gamaldo, S. M. Harding, R. M. Lloyd, S. F. Quan, M. T. Troester, and B. V. Vaughn. 2017. *The AASM Manual for the Scoring of Sleep and Associated Events: Rules, Terminology and Technical Specifications*. American Academy of Sleep Medicine.

Brown, Peter. 2003. “Oscillatory Nature of Human Basal Ganglia Activity: Relationship to the Pathophysiology of Parkinson’s Disease.” *Movement Disorders: Official Journal of the Movement Disorder Society* 18 (4): 357–63.

Chen, Chieh-Wen, Yam‐ting Kwok, Yu-Ting Cheng, Yu-Shan Huang, T. Kuo, Cheng-Han Wu, Pei-Jing Du, A. Yang, and Cheryl C. H. Yang. 2023. “Reduced Slow-Wave Activity and Autonomic Dysfunction during Sleep Precede Cognitive Deficits in Alzheimer’s Disease Transgenic Mice.” *Scientific Reports* 13 (July). https://doi.org/10.1038/s41598-023-38214-6.

Chen, Chiung Chu, Yi Ting Hsu, Hsiao Lung Chan, Shang Ming Chiou, Po Hsun Tu, Shih Tseng Lee, Chon Haw Tsai, Chin Song Lu, and Peter Brown. 2010. “Complexity of Subthalamic 13-35 Hz Oscillatory Activity Directly Correlates with Clinical Impairment in Patients with Parkinson’s Disease.” *Experimental Neurology* 224 (1): 234–40.

Chen, Jing, Danhua Zhao, Baoyu Chen, Qi Wang, Yuan Li, Junyi Chen, Chaobo Bai, et al. 2024. “Correlation of Slow-Wave Sleep with Motor and Nonmotor Progression in Parkinson’s Disease.” *Annals of Clinical and Translational Neurology* 11 (3): 554–63.

Di, Tianqi, Libo Zhang, Shiqiu Meng, Wangyue Liu, Yang Guo, Enyu Zheng, Chao Xie, et al. 2024. “The Impact of REM Sleep Loss on Human Brain Connectivity.” *Translational Psychiatry* 14 (1): 270.

Dumoulin Bridi, Michelle C., Sara J. Aton, Julie Seibt, Leslie Renouard, Tammi Coleman, and Marcos G. Frank. 2015. “Rapid Eye Movement Sleep Promotes Cortical Plasticity in the Developing Brain.” *Science Advances* 1 (6): e1500105.

Eusebio, Alexandre, Alek Pogosyan, Shouyan Wang, Bruno Averbeck, Louise Doyle Gaynor, Stéphanie Cantiniaux, Tatiana Witjas, Patricia Limousin, Jean-Philippe Azulay, and Peter Brown. 2009. “Resonance in Subthalamo-Cortical Circuits in Parkinson’s Disease.” *Brain: A Journal of Neurology* 132 (Pt 8): 2139–50.

Funk, Chadd M., Sakiko Honjoh, Alexander V. Rodriguez, Chiara Cirelli, and Giulio Tononi. 2016. “Local Slow Waves in Superficial Layers of Primary Cortical Areas during REM Sleep.” *Current Biology: CB* 26 (3): 396–403.

Gilron, Ro ’ee, Simon Little, Randy Perrone, Robert Wilt, Coralie de Hemptinne, Maria S. Yaroshinsky, Caroline A. Racine, et al. 2021. “Long-Term Wireless Streaming of Neural Recordings for Circuit Discovery and Adaptive Stimulation in Individuals with Parkinson’s

Disease.” *Nature Biotechnology* 39 (9): 1078–85.
González, David Andrés, Duo Wang, Erin Pollet, Angel Velarde, Sarah Horn, Pablo Coss, Okeanis Vaou, et al. 2024. “Performance of the Dreem 2 EEG Headband, Relative to Polysomnography, for Assessing Sleep in Parkinson’s Disease.” *Sleep Health* 10 (1): 24–30.
Hammond, Constance, Hagai Bergman, and Peter Brown. 2007. “Pathological Synchronization in Parkinson’s Disease: Networks, Models and Treatments.” *Trends in Neurosciences* 30 (7): 357–64.
He, Chao, Zhian Hu, and Chenggang Jiang. 2020. “Sleep Disturbance: An Early Sign of Alzheimer’s Disease.” *Neuroscience Bulletin* 36 (4): 449–51.
Irwin, Michael R., and Michael V. Vitiello. 2019. “Implications of Sleep Disturbance and Inflammation for Alzheimer’s Disease Dementia.” *Lancet Neurology* 18 (3): 296–306.
Ju, Yo-El S., S. Ooms, C. Sutphen, S. Macauley, Margaret A. Zangrilli, Gina Jerome, A. Fagan, et al. 2017. “Slow Wave Sleep Disruption Increases Cerebrospinal Fluid Amyloid-&bgr; Levels.” *Brain* 140 (August):2104–11.
Lee, Yee Fun, Dmitry Gerashchenko, Igor Timofeev, Brian J. Bacskai, and Ksenia V. Kastanenka. 2020. “Slow Wave Sleep Is a Promising Intervention Target for Alzheimer’s Disease.” *Frontiers in Neuroscience* 14 (June):705.
Little, Simon, and Peter Brown. 2014. “The Functional Role of Beta Oscillations in Parkinson’s Disease.” *Parkinsonism & Related Disorders* 20 Suppl 1 (January):S44–48.
Little, Simon, A. Pogosyan, A. A. Kuhn, and P. Brown. 2012. “β Band Stability over Time Correlates with Parkinsonian Rigidity and Bradykinesia.” *Experimental Neurology* 236 (2): 383–88.
Little, Simon, Huiling Tan, Anam Anzak, Alek Pogosyan, Andrea Kühn, and Peter Brown. 2013. “Bilateral Functional Connectivity of the Basal Ganglia in Patients with Parkinson’s Disease and Its Modulation by Dopaminergic Treatment.” *PloS One* 8 (12): e82762.
Moran, Rosalyn J., Nicolas Mallet, Vladimir Litvak, Raymond J. Dolan, Peter J. Magill, Karl J. Friston, and Peter Brown. 2011. “Alterations in Brain Connectivity Underlying Beta Oscillations in Parkinsonism.” *PLoS Computational Biology* 7 (8): e1002124.
Morelli, Nathan, and Rebekah L. S. Summers. 2023. “Association of Subthalamic Beta Frequency Sub-Bands to Symptom Severity in Patients with Parkinson’s Disease: A Systematic Review.” *Parkinsonism & Related Disorders* 110 (105364): 105364.
Musiek, Erik S., and David M. Holtzman. 2016. “Mechanisms Linking Circadian Clocks, Sleep, and Neurodegeneration.” *Science (New York, N.Y.)* 354 (6315): 1004–8.
Neumann, Wolf-Julian, Franziska Staub-Bartelt, Andreas Horn, Julia Schanda, Gerd-Helge Schneider, Peter Brown, and Andrea A. Kühn. 2017. “Long Term Correlation of Subthalamic Beta Band Activity with Motor Impairment in Patients with Parkinson’s Disease.” *Clinical Neurophysiology: Official Journal of the International Federation of Clinical Neurophysiology* 128 (11): 2286–91.
Oehrn, C., Stephanie Cernera, L. Hammer, Maria M. Shcherbakova, Jiaang Yao, Amelia Hahn, Sarah S. Wang, J. Ostrem, S. Little, and P. Starr. 2024. “Chronic Adaptive Deep Brain Stimulation versus Conventional Stimulation in Parkinson’s Disease: A Blinded Randomized Feasibility Trial.” *Nature Medicine*, August. https://doi.org/10.1038/s41591-024-03196-z.
Owen, Jessica E., and Sigrid C. Veasey. 2020. “Impact of Sleep Disturbances on Neurodegeneration: Insight from Studies in Animal Models.” *Neurobiology of Disease* 139 (104820): 104820.
Owen, Jessica E., Yan Zhu, P. Fenik, G. Zhan, P. Bell, Cathy Liu, and S. Veasey. 2021. “Late-in-Life Neurodegeneration after Chronic Sleep Loss in Young Adult Mice.” *Sleep* 44 (March). https://doi.org/10.1093/sleep/zsab057.
Porter, Verna R., William G. Buxton, and Alon Y. Avidan. 2015. “Sleep, Cognition and

Dementia." *Current Psychiatry Reports* 17 (12): 97.
Riedner, Brady A., Vladyslav V. Vyazovskiy, Reto Huber, Marcello Massimini, Steve Esser, Michael Murphy, and Giulio Tononi. 2007. "Sleep Homeostasis and Cortical Synchronization: III. A High-Density EEG Study of Sleep Slow Waves in Humans." *Sleep* 30 (12): 1643–57.
Rothman, Sarah M., and Mark P. Mattson. 2012. "Sleep Disturbances in Alzheimer's and Parkinson's Diseases." *Neuromolecular Medicine* 14 (3): 194–204.
Schenck, Carlos H., Bradley F. Boeve, and Mark W. Mahowald. 2013. "Delayed Emergence of a Parkinsonian Disorder or Dementia in 81% of Older Men Initially Diagnosed with Idiopathic Rapid Eye Movement Sleep Behavior Disorder: A 16-Year Update on a Previously Reported Series." *Sleep Medicine* 14 (8): 744–48.
Schreiner, Simon J., Lukas L. Imbach, Esther Werth, Rositsa Poryazova, Heide Baumann-Vogel, Philipp O. Valko, Tobias Murer, Daniela Noain, and Christian R. Baumann. 2019. "Slow-Wave Sleep and Motor Progression in Parkinson Disease." *Annals of Neurology* 85 (5): 765–70.
Shi, Le, Si-Jing Chen, Meng-Ying Ma, Yan-Ping Bao, Ying Han, Yu-Mei Wang, Jie Shi, Michael V. Vitiello, and Lin Lu. 2018. "Sleep Disturbances Increase the Risk of Dementia: A Systematic Review and Meta-Analysis." *Sleep Medicine Reviews* 40 (August):4–16.
Shokri-Kojori, Ehsan, Gene-Jack Wang, Corinde E. Wiers, Sukru B. Demiral, Min Guo, Sung Won Kim, Elsa Lindgren, et al. 2018. "β-Amyloid Accumulation in the Human Brain after One Night of Sleep Deprivation." *Proceedings of the National Academy of Sciences of the United States of America* 115 (17): 4483–88.
Smyth, Clay, Md Fahim Anjum, Shravanan Ravi, Timothy Denison, Philip Starr, and Simon Little. 2023. "Adaptive Deep Brain Stimulation for Sleep Stage Targeting in Parkinson's Disease." *Brain Stimulation* 16 (5): 1292–96.
Steriade, M., F. Amzica, and D. Contreras. 1996. "Synchronization of Fast (30-40 Hz) Spontaneous Cortical Rhythms during Brain Activation." *The Journal of Neuroscience: The Official Journal of the Society for Neuroscience* 16 (1): 392–417.
Stoffers, D., J. L. W. Bosboom, J. B. Deijen, E. Ch Wolters, C. J. Stam, and H. W. Berendse. 2008. "Increased Cortico-Cortical Functional Connectivity in Early-Stage Parkinson's Disease: An MEG Study." *NeuroImage* 41 (2): 212–22.
Tashjian, Sarah M., Diane Goldenberg, Martin M. Monti, and Adriana Galván. 2018. "Sleep Quality and Adolescent Default Mode Network Connectivity." *Social Cognitive and Affective Neuroscience* 13 (3): 290–99.
Tinkhauser, G., A. Pogosyan, S. Little, M. Beudel, D. Herz, H. Tan, and P. Brown. 2017. "The Modulatory Effect of Adaptive Deep Brain Stimulation on Beta Bursts in Parkinson's Disease." *Brain* 140 (February):1053–67.
Tinkhauser, G., A. Pogosyan, H. Tan, D. Herz, A. Kühn, and P. Brown. 2017. "Beta Burst Dynamics in Parkinson's Disease OFF and ON Dopaminergic Medication." *Brain : A Journal of Neurology* 140 (October):2968–81.
Uhlhaas, Peter J., and Wolf Singer. 2006. "Neural Synchrony in Brain Disorders: Relevance for Cognitive Dysfunctions and Pathophysiology." *Neuron* 52 (1): 155–68.
Verweij, Ilse M., Nico Romeijn, Dirk Ja Smit, Giovanni Piantoni, Eus Jw Van Someren, and Ysbrand D. van der Werf. 2014. "Sleep Deprivation Leads to a Loss of Functional Connectivity in Frontal Brain Regions." *BMC Neuroscience* 15 (1): 88.
Wisor, J., Michelle A. Schmidt, and William C. Clegern. 2011. "Evidence for Neuroinflammatory and Microglial Changes in the Cerebral Response to Sleep Loss." *Sleep* 34 (3): 261–72.
Wunderlin, Marina, Marc Alain Züst, Kristoffer Daniel Fehér, Stefan Klöppel, and Christoph Nissen. 2020. "The Role of Slow Wave Sleep in the Development of Dementia and Its Potential for Preventative Interventions." *Psychiatry Research. Neuroimaging* 306 (111178): 111178.

Xie, Lulu, Hongyi Kang, Qiwu Xu, Michael J. Chen, Yonghong Liao, Meenakshisundaram Thiyagarajan, John O'Donnell, et al. 2013. "Sleep Drives Metabolite Clearance from the Adult Brain." *Science (New York, N.Y.)* 342 (6156): 373–77.

Zahed, Hengameh, Jose Rafael Pantoja Zuzuarregui, Ro 'ee Gilron, Timothy Denison, Philip A. Starr, and Simon Little. 2021. "The Neurophysiology of Sleep in Parkinson's Disease." *Movement Disorders: Official Journal of the Movement Disorder Society* 36 (7): 1526–42.

Zielinski, Mark R., and Allison J. Gibbons. 2022. "Neuroinflammation, Sleep, and Circadian Rhythms." *Frontiers in Cellular and Infection Microbiology* 12 (March):853096.